HHS Public Access

Author manuscript

J Neurophysiol. Author manuscript; available in PMC 2015 April 30.

Published in final edited form as:

J Neurophysiol. 2006 November ; 96(5): 2528–2538. doi:10.1152/jn.00645.2006.

Spatiotemporal Patterns of an Evoked Network Oscillation in Neocortical Slices: Coupled Local Oscillators

Li Bai[1,2,*], **Xiaoying Huang**[1,*], **Qian Yang**[1], and **Jian-young Wu**[1]

[1]Department of Physiology and Biophysics, Georgetown University Medical Center, Washington, DC 20057

[2]Department of Cell and Molecular Immunology, Medical School, Henan University, Kaifeng 475001, China

Abstract

We have discovered an evoked network oscillation in rat neocortical slices and have examined its spatiotemporal patterns with voltage sensitive dye imaging. The slices (visual and auditory cortices) were prepared in a medium of low calcium, high magnesium and with sodium replaced by choline in order to reduce the excito-toxicity and sodium loading. After slicing, the choline was washed out while normal calcium, magnesium and sodium concentrations were restored. The oscillation was evoked by a single electrical shock to slices bathed in normal artificial cerebral spinal fluid (ACSF). The oscillation was organized as an all-or-none epoch containing 4 to 13 cycles at a central frequency around 25 Hz. The activity can be reversibly blocked by CNQX, APV and atropine, but not by bicuculline, indicating poly-synaptic excitatory mechanisms. Voltage sensitive dye imaging showed high amplitude oscillation signals in superficial and middle cortical layers. Spatiotemporally, the oscillations were organized as waves, propagating horizontally along cortical laminar. Each oscillation cycle was associated with one wave propagating in space. The waveforms were often different at different locations (e.g., extra cycles), suggesting the co-existence of multiple local oscillators. For different cycles, the waves often initiated at different locations, suggesting that local oscillators are competing to initiate each oscillation cycle. Overall our results suggest that this cortical network oscillation is organized at two levels: locally, oscillating neurons are tightly coupled to form local oscillators, and globally the coupling between local oscillators is weak, allowing abrupt spatial phase lags and propagating waves with multiple initiation sites.

Keywords

Voltage sensitive dye; gamma oscillations; optical recording; propagating waves

Corresponding Author: Jian-young Wu, Georgetown University, The Research Building, WP26, 3900 Reservoir Rd. NW, Washington, DC 20057, Phone: (202) 687-1614, Fax: (202) 687-0617, wuj@georgetown.edu.

*These authors contributed equally to this work

INTRODUCTION

Network oscillations of 20–80 Hz are widely observed in the cortex (Gray and Singer, 1989; Llinas and Ribary, 1993; Steriade et al., 1993; Tank et al., 1994; Franowicz and Barth, 1995; Nicolelis et al., 1995; Murthy and Fetz, 1996; Freeman and Barrie, 2000). Spatially organized oscillations may play a role in cortical processing such as sensory binding (Gray et al., 1989; Engel et al., 1991; Eckhorn, 1994, Buzsaki et al., 2002), coding sensory information or experience (Freeman and Viana di Prisco, 1986; Bressler, 1988; Chabaud et al., 2000) and attention (Fries et al., 2001). Since all of these neuronal processes are distributed in large areas of the cortex, studying the spatiotemporal patterns of the cortical oscillations is important in the understanding of how population neuronal activity is organized during these processes.

Many network oscillations are spatiotemporally organized as propagating waves (a.k.a. “traveling waves”, Ermentrout and Kleinfeld, 2001). Propagating waves have been observed during sensory processing including visual (Arieli et al., 1995,1996; Prechtl et al., 1997, 2000; Senseman and Robbins, 1999), somatosensory (Nicolelis et al., 1995, Petersen et al., 2003, Neuron paper 2006) and olfactory (Freeman and Barrie, 2000; Lam et al., 2000, 2003; Friedrich and Korsching, 1997). A possible mechanism for creating propagating waves is spatial distribution of phase gradient of coupled local oscillators (Kopell and Ermentrout, 1986; Cohen 1988; Ermentrout and Kleinfeld 2001). In a distributed network such as neocortex, a local oscillator can be defined as a group of tightly coupled oscillating neurons. Between two local oscillators, the coupling is relatively weak, allowing large phase lags to occur. The existence of such cortical local oscillators has been suggested by multi-electrode recordings from turtle visual cortex (Prechtl et al., 2000). However, many basic questions regarding cortical local oscillators have not been explored, e.g., what is the physical size of a local oscillator (single column/multiple columns) and whether these local oscillators are dynamically organized during each cortical event. The first step to approach these questions would be to visualize local oscillators with voltage-sensitive dye imaging. During a network oscillation local oscillators may be identified when large and abrupt phase lags occur between neighboring areas.

We have previously imaged two types of 4 – 15 Hz oscillations (Wu et al., 1999; Bao and Wu, 2003; Huang et al., 2004) and found phase variations between local areas (Bao and Wu 2003), suggesting the existence of local oscillators during these oscillations. However, large and abrupt phase lags were not seen, probably because the coupling among the local oscillators was too strong. We have also imaged an evoked oscillation of 20–80 Hz in neocortical slices (Wu et al., 2001). The oscillation can be recorded in local field potential, suggesting that oscillating neurons near the electrode tip formed tightly-coupled local oscillators. However, the oscillation can not be recorded by voltage-sensitive dye imaging, probably because the coupling on a local scale (under each optical detector) was too weak (Wu et al., 2001).

Along the line of effort for visualizing local oscillators in neocortex, we are searching for a cortical oscillation with strong coupling within a local oscillator and weak coupling between local oscillators. Here we report a discovery of an evoked network oscillation in neocortical

slices with this feature. Voltage-sensitive dye imaging revealed high amplitude oscillations, suggesting a strong local synchrony. At different locations the waveforms were different, suggesting weak coupling between local oscillators. In addition, different oscillation cycles often initiated from different locations, suggesting a competition between local oscillators to initiate each oscillation cycle. Our results suggest the oscillation is organized at two levels, locally neurons are more synchronized to form local oscillators but globally coupling between local oscillators are weak, allowing spatial distribution of phase lags and propagating waves.

MATERIALS AND METHODS

Cortical slice

Sprague-Dawley rats (n= 29) of both sexes from P21 to P32 were used in the experiments. Following NIH guidelines, the animals were deeply anesthetized with halothane and decapitated. The whole brain was quickly removed and chilled in cold (0–4 °C) slicing artificial CSF (sACSF) for 90 seconds. The sACSF contained (in mM), Choline chloride, 110; KCl, 2.5; $CaCl_2$, 0.5; $MgSO_4$, 7; NaH_2PO_4, 1.2; $NaHCO_3$, 25; dextrose 20; sucrose 10; L-ascorbic acid 1.3 and Na pyruvate 2.4 (modified from Hoffman and Johnston 1998) and the solution was bubbled with 95% O_2, 5% CO_2. Coronal slices (400 μm thick) of the whole cortical hemisphere were cut in the sACSF at 0 – 4 °C with a vibratome stage (752M Vibroslice, Campden Instruments, Sarasota, FL) and transferred into a holding chamber containing sACSF at 35 °C (bubbled vigorously with 95% O_2, 5% CO_2). After ~30 min incubation at 35 °C, the temperature was reduced to 26 °C (room temperature). Then half of the sACSF in the holding chamber was replaced by normal artificial CSF (ACSF, containing (in mM) NaCl, 132; KCl, 3; $CaCl_2$, 2; $MgSO_4$, 2; NaH_2PO_4, 1.25; $NaHCO_3$, 26; dextrose 10). The slices were then incubated in a combination of 1/2 sACSF and 1/2 ACSF for 2 to 3 hours until transferred to a submerged chamber for recording. The slice was perfused with ACSF at a rate of > 20 ml/min for at least 40 min (30 – 31 °C) in the submerged chamber before recording. In some experiments, the slices were cut horizontally, parallel to the cortical lamina (tangential slices) as described in our previous paper (Huang et al., 2004). These tangential slices were cut at 100 μm below the cortical surface and about 500 μm thick, contained most of the layers II–III and part of layer IV. Due to the curvature of the cortex, the size of the tangential slices were limited to about 4 × 6 mm^2.

Voltage-sensitive dye Imaging

The imaging apparatus and methods are described in detail in Jin et al. (2002). Briefly, the slices were stained for 60 min with ACSF containing 0.005 to 0.02 mg/ml of an oxonol dye, NK3630 (first synthesized by R. Hildesheim and A. Grinvald as RH482; available from Nippon Kankoh-Shikiso Kenkyusho Co., Ltd., Japan; See Momose-Sato et al. (1999) for molecular structure). After staining, the slices were washed in dye free ACSF for at least 30 min before recording and perfused in ACSF during imaging experiments. Voltage sensitive dye imaging was performed by a 124-element photodiode array (Centronics Inc., Newbury Park, CA) or a 464-element photodiode array (WuTech instruments; www.wutech.com). The imaging devices allow us to measure small signals (10^{-5}) at a fast (1600 frame/sec) imaging rate. Image of the tissue was projected by an objective of 5x (0.12 NA, dry lens,

Zeiss) or 20x (0.5NA, water immersion, Zeiss) to the diode array and each photodetector received light from an area of 0.33 × 0.33 mm^2 (5x) or 0.08 × 0.08 mm^2 (20x) of the cortical tissue respectively when the 124 array was used, and 0.13 × 0.13 mm^2 (5x) when the 464 array was used. The preparation was trans-illuminated by 705 ± 20 nm light and was only exposed to the illumination light during optical recording trials, for about 3 seconds per trial and less than 64 trials per slice. With this level of exposure, photodynamic damage and dye bleaching are not detectable (Jin et al., 2002). The voltage sensitive dye signal of the oscillation was about 10^{-4} (peak-to-peak) of the resting light intensity. Optical signal from each detector was individually amplified to 200×, low-pass filtered at 333 Hz and then multiplexed and digitized at 12 bits and 1,600 samples/sec per channel. A commercial version of 464 diode array is available as NeuroPDA from RedshirtImaging (www.redshirtimaging.com). Additional details about the imaging methods are discussed in Wu and Cohen (1993) and Jin et al. (2002).

Local field potential recordings

Tungsten epoxy-coated microelectrodes with tip resistance of ~75kΩ (FHC, Bowdoinham, ME) were used for stimulating and for recording local field potentials simultaneously with optical recordings. The field potential signals were amplified to 1000x and band-pass filtered between 0.1 to 400 Hz by a Brownlee Precision 440 amplifier. During imaging experiments, the field potential was digitized simultaneously with voltage sensitive dye signals at a rate of 1600 Hz. In some experiments, the slices were not stained and imaging was not performed, the oscillations were only recorded by local field potential electrodes. The LFP signals were recorded by a tape recorder (InstruTech Corp, Great Neck, NY) and digitized at 1600 Hz off-line. The LFP signals in stained and unstained slices were undistinguishable, suggesting that staining and voltage sensitive dye imaging did not contribute to the formation and sustaining of the oscillations.

Data analysis

The oscillation frequency was calculated by a program written in MatLab using the FFT function. The averaged frequency-power spectrum was obtained by adding the FFT of individual trials.

The optical data were analyzed using the program NeuroPlex (RedShirtImaging, LLC, Fairfield, CT) and displayed in the form of traces and pseudocolor images. To generate pseudocolor maps, the signals from each individual detector were normalized to their own maximum amplitude (peak =1 and baseline/negative peak =0), (Variable scaling in NeuroPlex). Then a scale of 16 colors was linearly assigned to the values between 0 and 1. The propagating velocity was calculated by dividing the distance between two locations by the time difference for a wave to reach these two locations.

RESULTS

The oscillation was accidentally discovered in the neocortical slices undergoing a procedure of reducing the excito-toxicity and sodium loading. In the procedure, sodium in the ACSF was replaced by choline during slicing (Hoffman and Johnston 1998). After slicing, the

sodium concentration was gradually restored while choline removed over a period of several hours in the holding chamber. The oscillations were evoked in normal ACSF after choline was thoroughly washed out. During experiment, the slices were continuously perfused with choline free ACSF at 30 – 31°C in a submerged chamber.

Field potential signals

The oscillation was evoked by a single electrical shock to cortical layers II–IV of slices from temporal cortex (area I–III, auditory cortex, Figure 1A) or occipital cortex (visual areas). Local field potential signals can be recorded from cortical layer II–III, at about 2 mm lateral to the stimulation site (Figure 1A, B). A shock of moderate intensity (~5V × 0.25 ms pulse, 1.5 times of the field potential response threshold) was enough to trigger an epoch of oscillations (Figure 1B). The oscillation epoch was an all-or-none event. Changing the stimulation intensity above the threshold did not alter the occurrence of the oscillation and the frequency, amplitude or the number of cycles in the epoch. With an inter-stimuli-interval of 30 seconds, the oscillation can be reliably evoked for at least 4 hours (68 slices from 29 animals). Each oscillation epoch started with a first spike and followed by 4 to 13 cycles of oscillations (Figure 1B, C). The first spike was more robust than the subsequent oscillation cycles. In a small fraction of trials, only the first spike was evoked and the subsequent oscillations failed to develop (Data not shown). While the number of cycles varied in different epochs (Figure 1C), the oscillation frequency was stable with small trial-to-trial variations (Figure 1D). The power spectrum (FFT) had a sharp frequency peak and the frequency peaks from multiple epochs were clustered together (Figure 1D). Sharp frequency peaks and small trial-to-trial variations suggest a stable organization of oscillating neurons near the electrode tip. However, the organization was only stable for a short time, about 4 – 13 cycles (Figure 1C).

Optical signals of the oscillation

Before optical recording, the slices were stained with voltage sensitive dye NK 3630. Local field potential recordings from stained and unstained slices did not noticeably differ in the amplitude, frequency and the number of oscillation cycles. Optical recording was done with a trans-illumination arrangement, and absorption of the stained tissue through the light path was measured. The optical signal at 705 ± 10 nm [on one side of the absorption peak of cortical tissue stained with NK 3630, Momose-Sato et al. (1999); Jin et al., (2002)] had both slow and fast components following the stimulus (Figure 2, trace 2). The slow component was independent of the illumination wavelength (Figure 2, trace 3), indicating that it was an “intrinsic” optical signal, or activity related light scattering due to cell swelling and shrinkage in the extracellular space (Sato et al., 1997; Jin et al., 2002; MacVicar, 2000). The fast component had a reversed polarity at 670 nm (data not shown), indicating that it was a voltage-sensitive dye signal, associated with membrane potential changes from the neurons stained with the voltage-sensitive dye (Ross et al., 1977; Jin et al., 2002). At 705 nm, the amplitude of the voltage-sensitive dye signal for the first spike was $5.2 \times 10^{-4} \pm 0.4 \times 10^{-4}$ (n= 143 trials from 7 slices) of resting light intensity. The intrinsic optical signal was about $8.6 \times 10^{-4} \pm 1.0 \times 10^{-4}$ (n=16 trials from 1 slice).

The voltage sensitive dye signals are correlated well with the field potential signals (Figure 2, traces 1–2), while the light scattering signal was too slow to follow the oscillation cycles (Figure 2, trace 3). Applying bicuculline (antagonist of $GABA_A$ receptors) significantly increased the amplitude of the light scattering signal and the amplitude of the first spike in the voltage sensitive dye signal (Figure 2, trace 4), suggesting that a larger fraction of neurons was activated in the first spike after the bicuculline disinhibition. However, the voltage sensitive dye signal of the subsequent oscillation cycles did not increase after bicuculline application, suggesting that the fraction of the oscillating neurons did not change after the $GABA_A$ inhibition was removed.

Laminar distribution of the oscillation

Voltage sensitive dye imaging revealed that the oscillations had large amplitude in superficial and middle cortical layers. Using a 20x microscope objective, we imaged the oscillations with ~100 detectors in a field of view of 1 mm in diameter, over the middle and deep layers of the cortex (Figure 3, left). Along the vertical axis from layers II–III to VI, there were 12 rows of optical detectors. The first spike was seen in all cortical layers. The amplitude of the subsequent oscillation cycles, however, decreased in the deep layers of the cortex (Figure 3, right). The amplitude reduction in deep layers was disproportional between the first spike and the subsequent oscillation cycles (Figure 3, right). In tangential slices containing only layers II-IV, oscillations occur normally (example traces shown in Figure 7B), suggesting that the oscillations can be sustained without deep layers.

Horizontal Propagation

Associated with each oscillation cycle a wave propagated horizontally (parallel to cortical laminar) in coronal slices (Figure 4, right). The propagation velocity was 0.045 ± 0.008 m/s (measured from 23 trials in slices from 2 animals). This velocity was slower than axonal conductance in cortex, suggesting that the wave was mediated by multiple synapses in the local circuit.

The propagation direction during different oscillation cycles was not fixed. Figure 4 shows two example trials recorded optically in the same tissue. The first trial had 4 cycles (Figure 4, top traces, cycles 1–3 and *s*) following the first spike (*f*). Cycles 1–3 reached detector A earlier than detector B, indicating that all propagated from medial to lateral (last cycle *s* had low amplitude and direction was indeterminate). The second trial was recorded a few seconds later and had 5 cycles following the first spike (Figure 4 bottom traces). In this trial, the first spike and the first two cycles of oscillation had the same propagation direction from medial to lateral, as in the first trial. But in the third cycle (*s*), the wave appeared simultaneously on both detectors and the subsequent two cycles (r1 and r2) had a reversed propagation direction. Change in propagation direction was seen in many optically recorded trials (further examined below), suggesting that different oscillation cycles started at different locations.

Initiation foci of the waves

In order to explain why different oscillation cycles often had different propagating directions, we examined oscillations with a 464-element diode array with higher spatial

resolution (128 μm diameter per detector). This high spatial resolution allowed us to more accurately locate the initiation site of the propagating wave associated with each oscillation cycle. In all trials recorded optically, the first spike always started at the location of stimulating electrode. The following oscillation cycles initiated at different locations. In the example shown in Figure 5, there were 7 oscillation cycles following the first spike. The first spike initiated at the location of the stimulating electrode (Figure 5, black cross in first top row image) and propagated across the slice. Two oscillation cycles, 3 and 7 initiated from two different locations (Figure 5, black crosses in middle and bottom row images) and propagated in a concentric pattern surrounding their initiation foci. Thus the variation in propagation directions shown in Figure 4 can be explained as two cycles starting from different locations.

We then examined whether oscillation cycles were initiated from a few preferred foci. In one slice, we have imaged 352 oscillation cycles and identified the initiation focus for each cycle. The initiation foci were defined as the location of the optical detector with earliest onset time (the time at which signal reached half of the maximum amplitude). We found that the majority of the initiation foci were distributed in the upper and middle layers of the Te III area (Figure 6A, right panel). Many cycles started from a few locations, indicating there were preferred initiation foci. Figure 6B shows the initiation foci for four example trials. In all four trials, the first spike was initiated at the location of stimulation (*F*). Subsequent oscillation cycles following the first spike were initiated at different locations, apparently in a random sequence for each epoch. The phenomenon of multiple initiation foci may be explained as a result of multiple local oscillators in the tissue. These local oscillators have similar frequency and compete to initiate each propagating wave. The existence of multiple local oscillators is also supported by evidence that the waveforms at different locations are significantly different (Two examples shown in the next section).

Multiple local oscillations

Imaging revealed a large variation in the waveform at different locations. Figure 7 shows two examples from slices sectioned in coronal and tangential planes. In both preparations, the waveforms at different locations were different. In the example shown in Figure 7A, the duration of the oscillations were similar in all locations, but two extra cycles were seen on detector 2 following the first spike (trace 2, arrowhead). Similarly, on detector 4 an extra cycle was seen at the end of the oscillation epoch (trace 4 arrowhead). Trials with waveform variations were often seen in recordings with high spatial resolution (51%, n=130 trials using the 464 array).

In tangential slices, the spatial variation in waveforms can be examined in the horizontal plane. Again a single shock evoked oscillations in a large area (marked by dashed line on the Figure 7B left), but within the area, individual detectors show different numbers of cycles and phases (Figure 7B, traces 1–4). The spatial average of the entire oscillating area (about 160 detectors, marked by dashed line in Figure 7B left,) showed a net depolarization with small oscillations (Figure 7B bottom trace), indicating that the oscillations were not synchronized over space. On the other hand, the local oscillators were not completely independent as indicated by the propagating waves accompanying each oscillation cycle (if

the oscillators were independent, then there would be no propagating waves). Movies from two examples, one from a coronal slice and another from a tangential slice, are presented as supplement movies 1 and 2 to demonstrate the irregularities of the propagating waves.

Pharmacological manipulations

The oscillation in this report only occurs in slices pre-treated with choline and choline needs to be thoroughly washed out before the oscillations can be triggered. Slices prepared by another method, using sucrose to replace NaCl (Sanchez-Vives and McCormick, 2000), did not show this evoked oscillation. Apparently, Choline modifies the local cortical circuits during slicing and subsequent incubation when sodium concentration was restored.

Synaptic mechanisms of the oscillation were explored with agonists and antagonists of common neurotransmitters. Figure 8 summarizes the effects of blocking major neocortical synapses. Antagonists to the N-methyl-D-aspartate (NMDA) subtype glutamate receptors, 2-amino-5-phosphonopentanoic acid (APV) reversibly blocked the oscillation (Figure 8A). Increasing the concentration of Mg^{++} in the ACSF, from normal 2 mM to 3 – 4 mM also reversibly blocked the oscillation (Figure 8B). In high Mg^{++} media it became more difficult to evoke the oscillation with the same stimulation intensity, and the failure rate of evoking the oscillation become higher (Figure 8B middle trace). Blocking AMPA subtype receptors by their antagonist 6-cyano-7-nitroquinoxaline-2,3-dione (CNQX) also blocked the oscillations (Figure 8C). Perfusing with $GABA_A$ receptor antagonist bicuculline did not block the oscillations. The amplitude of the first spike and the number of oscillation cycles increased with bicuculline (Figure 2, trace 4; Figure 8D). Manipulating muscarinic cholinergic receptors also affected the oscillations. The oscillations were sensitive to muscarinic receptor antagonist atropine (completely blocked in 10 μM, Figure 8E). Carbachol, a muscarinic/nicotinic receptor agonist, also blocked the oscillations at a low concentration (~10 μM, Figure 8F). In contrast, nicotinic receptor antagonist methyllycaconitine (100 nM) had no apparent effect on the oscillation (neither enhancing nor blocking, data not shown).

Taken together, the pharmacological profile of the oscillation can distinguish it from other known oscillations in rat neocortical and hippocampal slices.

DISCUSSION

The principal findings of this report are that (1) a new type of evoked oscillation in rat neocortical slices was discovered, with distinct pharmacological characteristics from other known oscillations in rat cortical slices, (2) the oscillation manifests as propagating waves and the waveforms are different at different locations, (3) different oscillation cycles often initiate from different locations, suggesting a competition between local oscillators to be the pacemaker for each cycle.

Synchrony of oscillating neurons on local scale

Voltage sensitive dye imaging provides a useful tool for examining the spatiotemporal patterns of oscillations in cortical network. The amplitude of the voltage sensitive dye signal can be used to estimate the fraction of neurons synchronized in a local oscillating

population. The voltage sensitive dye signal is linearly correlated to transmembrane potentials (Ross et al., 1977) and the sensitivity of the voltage sensitive dye is comparable to local field potential microelectrodes in measuring cortical population neuronal activities (Jin et al., 2002). In our absorption dye measurement, all neurons 'seen' by each optical detector contributed relatively equally to the voltage sensitive dye signal, thus the amplitude of the voltage sensitive dye signal reflects a net sum of the membrane potential fluctuation of all neurons under each detector. Large voltage sensitive dye signals of the oscillations (Figure 2 – 7) indicate that a large fraction of oscillating neurons is synchronized on a local scale, under each optical detector. The density of cortical neurons was estimated to be about 100,000 neurons/mm^3 (Douglas and Martin, 1991) and the tissue volume projected onto each optical detector (of the 128 array) contains about 5,000 neurons. During an all-or-none epileptiform event under bicuculline disinhibition (aka interictal-like spike), about 80% of the neurons are activated (Wu et al., 2001). Trace 4 of Figure 2 shows that with bicuculline the amplitude of the first spike is similar to that of interictal-like spikes, and that the first spike is about 3 times larger than other oscillation cycles. Thus we estimate that about 30% of the local population is synchronized during the oscillations. Intrinsic optical signals were about twice as large in the presence of bicuculline as that in normal ACSF, consistent with the estimation that a smaller fraction of neurons is synchronized during oscillations than during an all-or-none epileptiform event (trace 3 and 4 of Figure 2).

Local oscillators

As mentioned above, large voltage sensitive dye signals indicate synchrony among the oscillating neurons on a local scale under each detector. Strong local synchrony was also suggested by the fact that the oscillation had a sharp frequency peak and the peak was robust from trial-to-trial.

If at two locations the oscillation waveforms are different, there must be two or more clusters of synchronized oscillating neurons (local oscillators). Different oscillating waveforms were often observed at different locations (Figure 7), indicating that multiple local oscillators co-exist simultaneously at different locations. However, with the present data we do not know if there is a sharp boundary between two neighboring local oscillators. This oscillation has another feature that different oscillation cycles often initiate from different locations (Figures 5, 6). Such switching of initiation sites also suggests the existence of multiple local oscillators. The oscillators may have a similar frequency and a weak coupling between each other. At the beginning of each oscillation cycle, the oscillators compete and the one with the earliest phase becomes the pacemaker to lead the wave. As a result, the propagation path has large cycle-to-cycle variations (Figure 4, 5, supplemental movies).

Comparison with other *in vitro* oscillations

In addition to the oscillation in this report, seven other kinds of oscillatory activity have been described in rat neocortical and hippocampal slices (I – VII, Table 1). Five of them, I – V have been examined with voltage sensitive dye imaging or an electrode array. The oscillation in this report is organized as propagating waves with a pattern of one oscillation cycle associating with one wave propagating in space (one-cycle-one-wave). The one-cycle-

one-wave pattern was also observed during oscillation types I (Wu et al., 1999), III (Bao and Wu, 2003; Huang et al., 2004) and V (Kim et al., 1995). In contrast, oscillation type II was synchronized over space and did not appear as propagating waves (Figure 3 of Mann et al., 2005). Compared to oscillation types I and III, the oscillation in this report had larger variations from cycle to cycle and more frequent switching of wave initiation sites, suggesting a weaker spatial coupling. The 20–80 Hz oscillations (type IV) can be seen in local field potential recordings, suggesting a certain level of local synchrony in the oscillating population. However, the oscillations cannot be seen in the voltage sensitive dye signals (Wu et al, 2001), suggesting that each small volume of tissue projected onto one optical detector contains multiple local oscillators. A spatial average of 160 detectors during the oscillation in this report can also create a mostly non-oscillatory waveform (Figure 7B right, bottom trace), consistent with the idea that a mixture of loosely coupled local oscillations results in a non-synchronized waveform.

Pharmacological profile can also distinguish the oscillation in this report from the other known oscillatory activity in cortical slices. The oscillation is mediated by excitatory synaptic connections with the involvement of both NMDA and AMPA receptors (Figure 8 A – C). Carbachol blocks the activity (Figure 8F), distinguishing it from oscillation types II and III that are induced by carbachol. Blocking $GABA_A$ mediated inhibitory circuits did not block the oscillation (Figure 8D), distinguishing it from oscillation types IV, V and VI. Overall, the frequency, duration, spatiotemporal pattern and pharmacological properties indicate that the oscillation in this report is different from other known oscillations induced in cortical and hippocampal slices.

Propagating waves

Propagating waves have been seen in cortical neuronal networks during both excitatory and oscillatory events. Excitatory waves in brain tissue have been examined extensively (Albowitz and Kuhnt 1995; Chervin et al., 1988; Grinvald et al., 1984; Tsau et al., 1998; Demir et al., 1998; Wu et al., 2001; Miyakawa et al., 2003; Tanifuji et al., 1994; Golomb and Amitai, 1997; Fleidervish et al., 1998). GABAergic inhibition is important for controlling the propagation of excitatory waves (Traub et al., 1987; Miles et al., 1988; Chagnac-Amitai and Connors, 1989; Wadman and Gutnick, 1993; Golomb and Ermentrout, 2002). When $GABA_A$ receptors are blocked with bicuculline, the excitation wave propagates at about 0.14 m/sec in hippocampal slices (Miles et al., 1988) and 0.08 m/sec (Chervin et al., 1988) to 0.13 m/sec (Wu et al., 2001) in neocortical slices. These excitatory waves are much faster than the oscillatory waves in this report.

Propagating waves also occur during oscillatory events. Spatial phase distribution among coupled oscillators is a mechanism for generating propagating waves (Ermentrout and Kleinfeld, 2001; Osan and Ermentrout, 2001). Experimentally distinguishing local oscillators in neuronal populations may be difficult if coupling over space is so strong that it diminishes the spatial phase shift between local oscillators. For example, carbachol induced oscillations in hippocampal slices (type II, table 1) do not propagate (Figure 3 of Mann et al., 2005), making it impossible to visualize individual oscillators. Carbachol induced oscillations in neocortical slices (type III, table 1) do propagate, but evidence for the

existence of local oscillators can only be found indirectly (Bao and Wu 2003). The oscillation in this report provides an example where spatial coupling is weak enough to identify local oscillators but strong enough to form propagating waves (Figure 5, Supplemental movies 1 and 2).

In the intact brain, propagating waves have been observed during oscillations evoked by natural sensory input (Freeman and Barrie, 2000; Dorries and Kauer, 2000; Prechtl et al., 1997, 2000; Senseman and Robbins, 1999; Lam et al., 2000). The one-wave-one-cycle pattern was also found *in vivo* by voltage sensitive dye imaging (Prechtl et al., 1997; Lam et al., 2003). Our analysis in this report suggests that complex wave patterns (as that seen *in vivo*, Lam et al., 2003) may be a result of weakly coupled local oscillations.

In conclusion, our results showed that the oscillation we have described here has two levels of spatiotemporal organization. On a local scale, a fraction of oscillating neurons is synchronized to form local oscillators, resulting in large amplitude voltage sensitive dye signals. On a global scale, the coupling between local oscillators is weak, resulting in variations of waveforms and propagating paths. Further experiments are needed to examine the size of the local oscillators and the factors controlling the spatial coupling on both local and global scales.

Acknowledgments

We are grateful to Drs. N. Cappaert, B. Tan and K. Takagaki for helpful discussions.

Supported by NIH NS036447 and a Whitehall Foundation grant

References

Albowitz B, Kuhnt U. Epileptiform activity in the guinea-pig neocortical slice spreads preferentially along supragranular layers–recordings with voltage-sensitive dyes. Eur J Neurosci. 1995; 7:1273–1284. [PubMed: 7582100]

Anderson WW, Lewis DV, Swartzwelder HS, Wilson WA. Magnesium-free medium activates seizure-like events in the rat hippocampal slice. Brain Res. 1986; 398:215–219. [PubMed: 3801897]

Arieli A, Shoham D, Hildesheim R, Grinvald A. Coherent spatiotemporal patterns of ongoing activity revealed by real-time optical imaging coupled with single-unit recording in the cat visual cortex. J Neurophysiol. 1995; 73:2072–2093. [PubMed: 7623099]

Arieli A, Sterkin A, Grinvald A, Aertsen A. Dynamics of ongoing activity: explanation of the large variability in evoked cortical responses. Science. 1996; 273:1868–1871. [PubMed: 8791593]

Bao W, Wu JY. Propagating wave and irregular dynamics: spatiotemporal patterns of cholinergic theta oscillations in neocortex in vitro. J Neurophysiol. 2003; 90:333–341. [PubMed: 12612003]

Bressler SL. Changes in electrical activity of rabbit olfactory bulb and cortex to conditioned odor stimulation. Behav Neurosci. 1988; 102:740–747. [PubMed: 3196442]

Buhl EH, Tamas G, Fisahn A. Cholinergic activation and tonic excitation induce persistent gamma oscillations in mouse somatosensory cortex in vitro. J Physiol. 1998; 513:117–126. [PubMed: 9782163]

Buzsaki G, Csicsvari J, Dragoi G, Harris K, Henze D, Hirase H. Homeostatic maintenance of neuronal excitability by burst discharges in vivo. Cereb Cortex. 2002; 12:893–899. [PubMed: 12183388]

Chabaud P, Ravel N, Wilson DA, Mouly AM, Vigouroux M, Farget V, Gervais R. Exposure to behaviourally relevant odour reveals differential characteristics in rat central olfactory pathways as studied through oscillatory activities. Chem Senses. 2000; 25:561–573. [PubMed: 11015328]

Chagnac-Amitai Y, Connors BW. Horizontal spread of synchronized activity in neocortex and its control by GABA-mediated inhibition. J Neurophysiol. 1989; 61:747–758. [PubMed: 2542471]

Chervin RD, Pierce PA, Connors BW. Periodicity and directionality in the propagation of epileptiform discharges across neocortex. J Neurophysiol. 1988; 60:1695–1713. [PubMed: 3143812]

Cohen, AH. Evolution of the vertebrate central pattern generator for locomotion. In: Cohen, AH.; Rossignol, A.; Grillner, S., editors. Neural Control of Rhythmic Movements in Vertebrates. Wiley & Sons; 1988. p. 129-166.

Cunningham MO, Davies CH, Buhl EH, Kopell N, Whittington MA. Gamma oscillations induced by kainate receptor activation in the entorhinal cortex in vitro. J Neurosci. 2003; 23:9761–9769. [PubMed: 14586003]

Demir R, Haberly LB, Jackson MB. Voltage imaging of epileptiform activity in slices from rat piriform cortex: onset and propagation. J Neurophysiol. 1998; 80:2727–2742. [PubMed: 9819277]

Dickinson R, Awaiz S, Whittington MA, Lieb WR, Franks NP. The effects of general anaesthetics on carbachol-evoked gamma oscillations in the rat hippocampus in vitro. Neuropharmacology. 2003; 44:864–872. [PubMed: 12726818]

Dorries KM, Kauer JS. Relationships between odor-elicited oscillations in the salamander olfactory epithelium and olfactory bulb. J Neurophysiol. 2000; 83:754–765. [PubMed: 10669491]

Douglas RJ, Martin KA. A functional microcircuit for cat visual cortex. J Physiol. 1991; 440:735–769. [PubMed: 1666655]

Eckhorn R. Oscillatory and non-oscillatory synchronizations in the visual cortex and their possible roles in associations of visual features. Prog Brain Res. 1994; 102:405–426. [PubMed: 7800830]

Engel AK, Kreiter AK, Konig P, Singer W. Synchronization of oscillatory neuronal responses between striate and extrastriate visual cortical areas of the cat. Proc Natl Acad Sci U S A. 1991; 88:6048–6052. [PubMed: 2068083]

Ermentrout GB, Kleinfeld D. Traveling electrical waves in cortex: insights from phase dynamics and speculation on a computational role. Neuron. 2001; 29:33–44. [PubMed: 11182079]

Fisahn A, Pike FG, Buhl EH, Paulsen O. Cholinergic induction of network oscillations at 40 Hz in the hippocampus in vitro. Nature. 1998; 394:186–189. [PubMed: 9671302]

Fleidervish IA, Binshtok AM, Gutnick MJ. Functionally distinct NMDA receptors mediate horizontal connectivity within layer 4 of mouse barrel cortex. Neuron. 1998; 21:1055–1065. [PubMed: 9856461]

Flint AC, Connors BW. Two types of network oscillations in neocortex mediated by distinct glutamate receptor subtypes and neuronal populations. J Neurophysiol. 1996; 75:951–957. [PubMed: 8714667]

Franowicz MN, Barth DS. Comparison of evoked potentials and high-frequency (gamma-band) oscillating potentials in rat auditory cortex. J Neurophysiol. 1995; 74:96–112. [PubMed: 7472356]

Freeman WJ, Viana Di Prisco G. Relation of olfactory EEG to behavior: time series analysis. Behav Neurosci. 1986; 100:753–763. [PubMed: 3778638]

Freeman WJ, Barrie JM. Analysis of spatial patterns of phase in neocortical gamma EEGs in rabbit. J Neurophysiol. 2000; 84:1266–1278. [PubMed: 10980001]

Friedrich RW, Korsching SI. Combinatorial and chemotopic odorant coding in the zebrafish olfactory bulb visualized by optical imaging. Neuron. 1997; 18:737–752. [PubMed: 9182799]

Fries P, Reynolds JH, Rorie AE, Desimone R. Modulation of oscillatory neuronal synchronization by selective visual attention. Science. 2001; 291:1560–1563. [PubMed: 11222864]

Golomb D, Amitai Y. Propagating neuronal discharges in neocortical slices: computational and experimental study. J Neurophysiol. 1997; 78:1199–1211. [PubMed: 9310412]

Golomb D, Ermentrout GB. Slow excitation supports propagation of slow pulses in networks of excitatory and inhibitory populations. Phys Rev E Stat Nonlin Soft Matter Phys. 2002; 65:061911. [PubMed: 12188763]

Gray CM, Konig P, Engel AK, Singer W. Oscillatory responses in cat visual cortex exhibit inter-columnar synchronization which reflects global stimulus properties. Nature. 1989; 338:334–337. [PubMed: 2922061]

Gray CM, Singer W. Stimulus-specific neuronal oscillations in orientation columns of cat visual cortex. Proc Natl Acad Sci U S A. 1989; 86:1698–1702. [PubMed: 2922407]

Grinvald A, Anglister L, Freeman JA, Hildesheim R, Manker A. Real-time optical imaging of naturally evoked electrical activity in intact frog brain. Nature. 1984; 308:848–850. [PubMed: 6717577]

Hoffman DA, Johnston D. Downregulation of transient K+ channels in dendrites of hippocampal CA1 pyramidal neurons by activation of PKA and PKC. J Neurosci. 1998; 18:3521–3528. [PubMed: 9570783]

Huang X, Troy WC, Yang Q, Ma H, Laing CR, Schiff SJ, Wu JY. Spiral waves in disinhibited mammalian neocortex. J Neurosci. 2004; 24:9897–9902. [PubMed: 15525774]

Jin W, Zhang RJ, Wu JY. Voltage-sensitive dye imaging of population neuronal activity in cortical tissue. J Neurosci Methods. 2002; 115:13–27. [PubMed: 11897360]

Kim U, Bal T, McCormick DA. Spindle waves are propagating synchronized oscillations in the ferret LGNd in vitro. J Neurophysiol. 1995; 74:1301–1323. [PubMed: 7500152]

Kopell N, Ermentrout GB. Symmetry and phaselocking in chains of weakly coupled oscillators. Comm Pure Aool Math. 1986; 39:623–660.

Lam YW, Cohen LB, Wachowiak M, Zochowski MR. Odors elicit three different oscillations in the turtle olfactory bulb. J Neurosci. 2000; 20:749–762. [PubMed: 10632604]

Lam YW, Cohen LB, Zochowski MR. Odorant specificity of three oscillations and the DC signal in the turtle olfactory bulb. Eur J Neurosci. 2003; 17:436–446. [PubMed: 12581162]

Llinas R, Ribary U. Coherent 40-Hz oscillation characterizes dream state in humans. Proc Natl Acad Sci U S A. 1993; 90:2078–2081. [PubMed: 8446632]

Lukatch HS, MacIver MB. Physiology, pharmacology, and topography of cholinergic neocortical oscillations in vitro. J Neurophysiol. 1997; 77:2427–2445. [PubMed: 9163368]

Luhmann HJ, Prince DA. Transient expression of polysynaptic NMDA receptor-mediated activity during neocortical development. Neurosci Lett. 1990; 111:109–115. [PubMed: 1970856]

MacVicar, BA. Intrinsic signal optical imaging in brain slices. In: Yuste, R.; Lanni, F.; Konnerth, A., editors. Imaging neurons a laboratory manual. New York: Cold Spring Harbor Laboratory Press; 2000. p. 47.1-47.7.

Mann E, Suckling JM, Hajos N, Greenfield SA, Paulsen O. Perisomatic Feedback Inhibition Underlies Cholinergically Induced Fast Network Oscillations in the Rat Hippocampus In Vitro. Neuron. 2005; 45:105–117. [PubMed: 15629706]

Metherate R, Cruikshank SJ. Thalamocortical inputs trigger a propagating envelope of gamma-band activity in auditory cortex in vitro. Exp Brain Res. 1999; 126:160–174. [PubMed: 10369139]

Miles R, Traub RD, Wong RK. Spread of synchronous firing in longitudinal slices from the CA3 region of the hippocampus. J Neurophysiol. 1988; 60:1481–1496. [PubMed: 3193167]

Miyakawa N, Yazawa I, Sasaki S, Momose-Sato Y, Sato K. Optical analysis of acute spontaneous epileptiform discharges in the in vivo rat cerebral cortex. Neuroimage. 2003; 18:622–632. [PubMed: 12667839]

Momose-Sato Y, Sato K, Arai Y, Yazawa I, Mochida H, Kamino K. Evaluation of voltage-sensitive dyes for long-term recording of neural activity in the hippocampus. J Membr Biol. 1999; 172:145–157. [PubMed: 10556362]

Murthy VN, Fetz EE. Oscillatory activity in sensorimotor cortex of awake monkeys: synchronization of local field potentials and relation to behavior. J Neurophysiol. 1996; 76:3949–3967. [PubMed: 8985892]

Nicolelis MA, Baccala LA, Lin RC, Chapin JK. Sensorimotor encoding by synchronous neural ensemble activity at multiple levels of the somatosensory system. Science. 1995; 268:1353–1358. [PubMed: 7761855]

Osan R, Ermentrout GB. Two dimensional synaptically generated traveling waves in a theta-neuron neural network. Neurocomputing. 2001:38–40. 789–795.

Petersen CC, Hahn TT, Mehta M, Grinvald A, Sakmann B. Interaction of sensory responses with spontaneous depolarization in layer 2/3 barrel cortex. Proc Natl Acad Sci U S A. 2003; 100:13638–13643. [PubMed: 14595013]

Prechtl JC, Cohen LB, Pesaran B, Mitra PP, Kleinfeld D. Visual stimuli induce waves of electrical activity in turtle cortex. Proc Natl Acad Sci U S A. 1997; 94:7621–7626. [PubMed: 9207142]

Prechtl JC, Bullock TH, Kleinfeld D. Direct evidence for local oscillatory current sources and intracortical phase gradients in turtle visual cortex. Proc Natl Acad Sci U S A. 2000; 97:877–882. [PubMed: 10639173]

Ross WN, Salzberg BM, Cohen LB, Grinvald A, Davila HV, Waggoner AS, Wang CH. Changes in absorption, fluorescence, dichroism, and Birefringence in stained giant axons: optical measurement of membrane potential. J Membr Biol. 1977; 33:141–183. [PubMed: 864685]

Sanchez-Vives MV, McCormick DA. Cellular and network mechanisms of rhythmic recurrent activity in neocortex. Nat Neurosci. 2000; 3:1027–1034. [PubMed: 11017176]

Sato K, Momose-Sato Y, Arai Y, Hirota A, Kamino K. Optical illustration of glutamate-induced cell swelling coupled with membrane depolarization in embryonic brain stem slices. Neuroreport. 1997; 8:3559–3563. [PubMed: 9427326]

Senseman DM, Robbins KA. Modal behavior of cortical neural networks during visual processing. J Neurosci. 1999; 19:RC3. [PubMed: 10234049]

Silva LR, Amitai Y, Connors BW. Intrinsic oscillations of neocortex generated by layer 5 pyramidal neurons. Science. 1991; 251:432–435. [PubMed: 1824881]

Steriade M, McCormick DA, Sejnowski TJ. Thalamocortical oscillations in the sleeping and aroused brain. Science. 1993; 262:679–685. [PubMed: 8235588]

Tanifuji M, Sugiyama T, Murase K. Horizontal propagation of excitation in rat visual cortical slices revealed by optical imaging. Science. 1994; 266:1057–1059. [PubMed: 7973662]

Tank DW, Gelperin A, Kleinfeld D. Odors, oscillations and waves: Does it all compute? Science. 1994; 265:1819–1820. [PubMed: 17797218]

Towers SK, LeBeau FE, Gloveli T, Traub RD, Whittington MA, Buhl EH. Fast network oscillations in the rat dentate gyrus in vitro. J Neurophysiol. 2002; 87:1165–1168. [PubMed: 11826085]

Traub RD, Knowles WD, Miles R, Wong RK. Models of the cellular mechanism underlying propagation of epileptiform activity in the CA2-CA3 region of the hippocampal slice. Neuroscience. 1987; 21:457–470. [PubMed: 3039403]

Tsau Y, Guan L, Wu JY. Initiation of spontaneous epileptiform activity in the neocortical slice. J Neurophysiol. 1998; 80:978–982. [PubMed: 9705483]

Wadman WJ, Gutnick MJ. Non-uniform propagation of epileptiform discharge in brain slices of rat neocortex. Neuroscience. 1993; 52:255–262. [PubMed: 8450945]

Whittington MA, Traub RD, Jefferys JG. Synchronized oscillations in interneuron networks driven by metabotropic glutamate receptor activation. Nature. 1995; 373:612–615. [PubMed: 7854418]

Wu, JY.; Cohen, LB. Fast multisite optical measurement of membrane potential. In: Mason, WT., editor. Fluorescent Probes for Biological Activity. New York: Academic Press; 1993.

Wu JY, Guan L, Tsau Y. Propagating activation during oscillations and evoked responses in neocortical slices. J Neurosci. 1999; 19:5005–5015. [PubMed: 10366633]

Wu JY, Guan L, Bai L, Yang Q. Spatiotemporal properties of an evoked population activity in rat sensory cortical slices. J Neurophysiol. 2001; 86:2461–2474. [PubMed: 11698535]

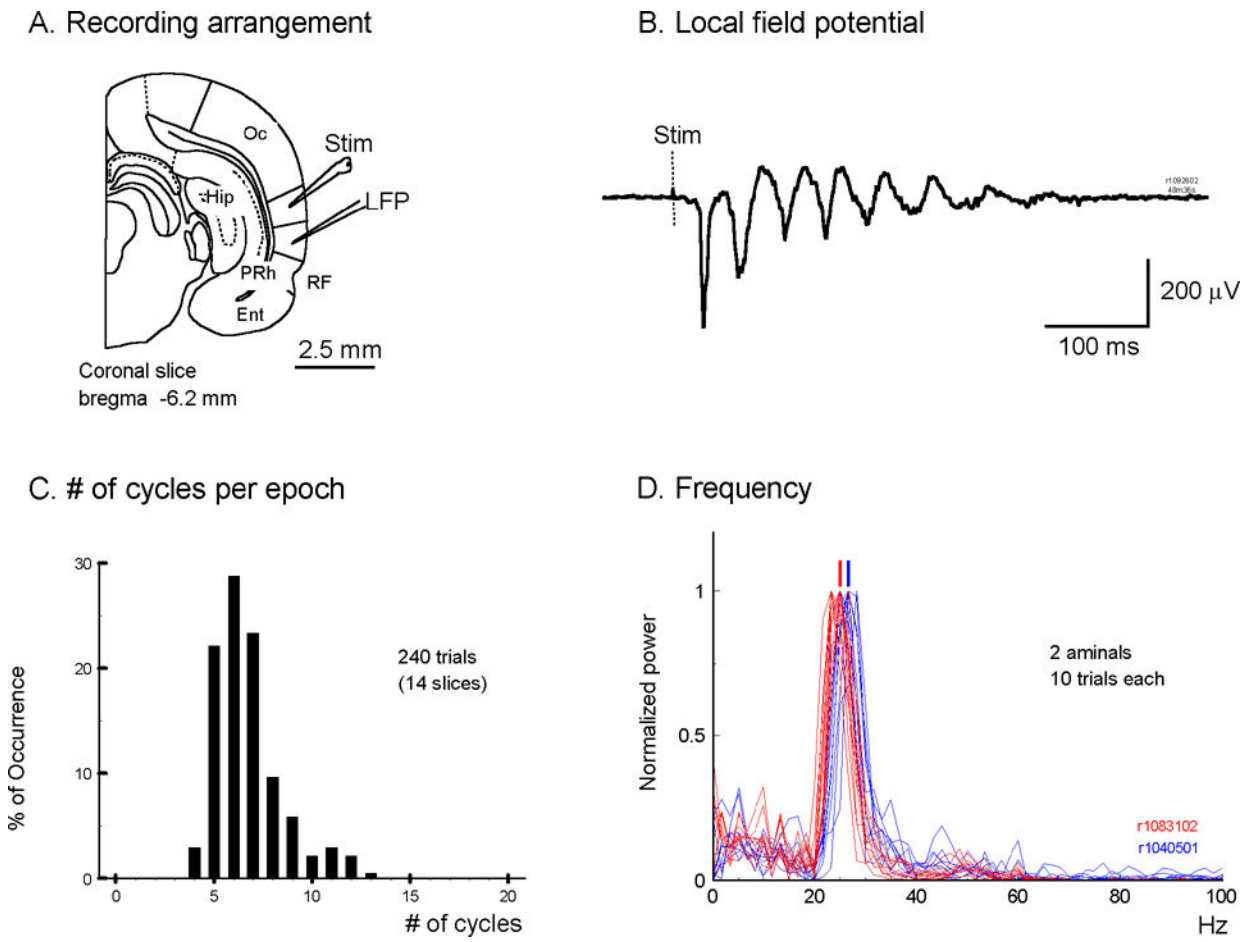

Figure 1.

A. The stimulation-recording arrangement. The stimulation and recording electrodes were placed in temporal areas II–III, 1 to 2 mm apart. ***B.*** An example of the oscillations recorded from a local field potential electrode. ***C.*** The distribution of the number of oscillation cycles in each epoch (n= 240 epochs recorded from 14 slices, not counting the first spike). ***D.*** The power spectrum (FFT) of oscillations recorded from two animals (red and blue, 10 epochs each). The short red bar and blue bar shows the average peak frequency of each animal respectively (red, 25 Hz; blue, 26.6 Hz). *Oc*, occipital cortex; *RF*, rhinal fissure; *PRh*, perirhinal cortex; *Ent*, entorhinal cortex; *Hip*, hippocampus.

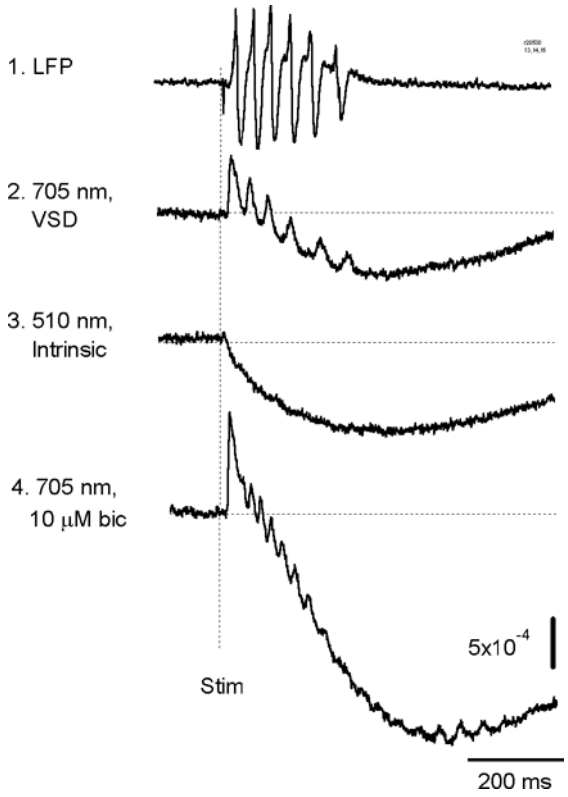

Figure 2.

Electrical and optical signals of the oscillation. Traces 1 and 2, simultaneous recording of local field potential (LFP) and optical signal from layer III, about 1 mm lateral to the stimulation site. Trace 3, optical signal at 510 nm of light from the same detector during another trial. Trace 4, optical signal from the same detector after the tissue was bathed with bicuculline. The optical signals were from one photo-detector which received light from an area of 83 × 83 μm (20x objective).

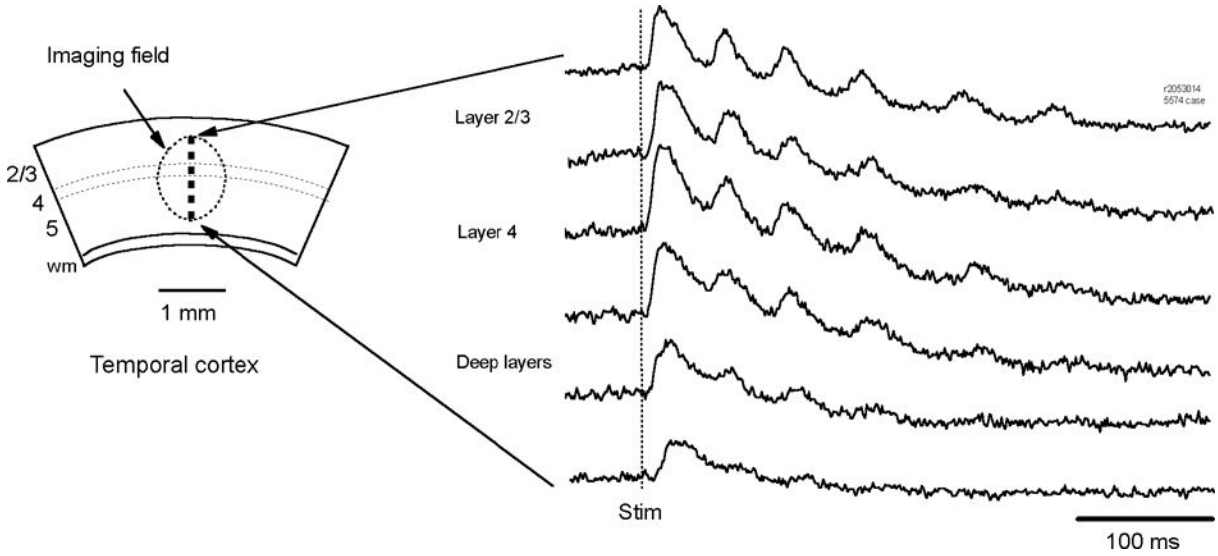

Figure 3.

Oscillation amplitude in different cortical layers. Voltage-sensitive dye signals (right traces) from 6 optical detectors imaging different cortical layers (left). The oscillation amplitude was high in Layer II-IV but low in deep layers. In contrast the first spike was seen in all the layers.

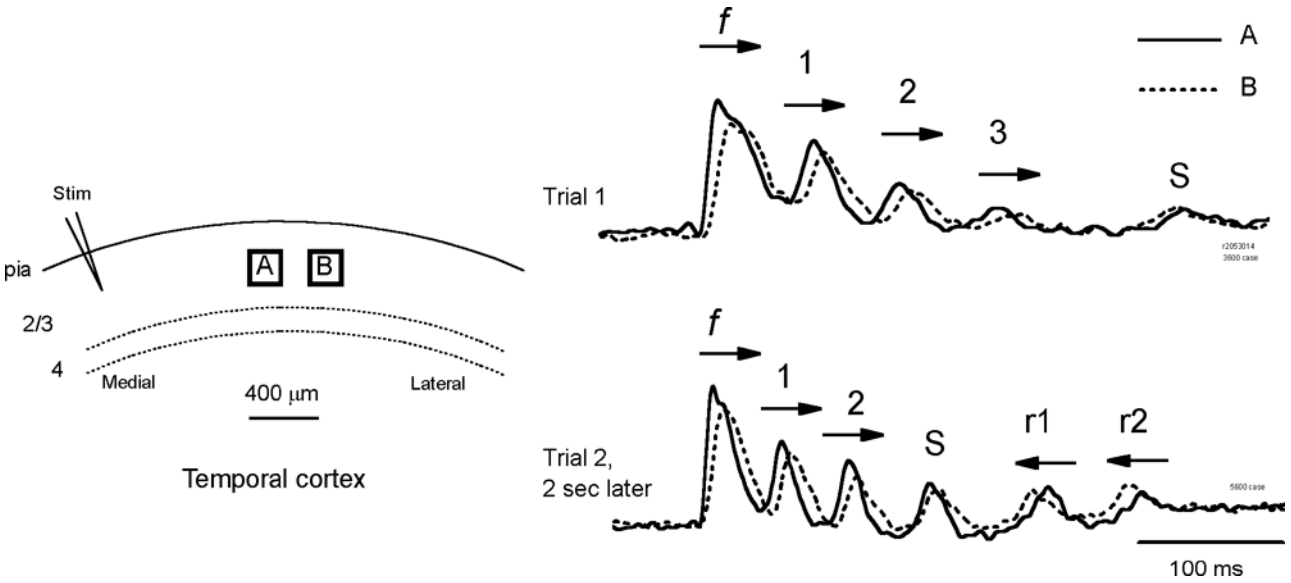

Figure 4.

Horizontal propagation of different oscillation cycles. **Left**: Optical detectors, A and B, are placed in layer II–III about 1.2 mm lateral to the stimulating electrode (Stim). **Right**: Optical signals from the two detectors are shown as solid (A) and broken lines (B) respectively, during two trials of evoked oscillations. Arrows on each cycle mark the horizontal propagation direction of the cycle. The direction was determined by the onset time for the waves arriving at the two detectors. The propagating direction of the first spike (*f*) was same for both trials, coming from the stimulation site and propagating to the lateral. In trial 1, three cycles following the first spike (1–3) had the same propagating direction, medial to lateral. At the end of trial 1 there may be another cycle (s) with direction indeterminate due to small amplitude. In trial 2 (evoked 2 seconds later) two cycles (1–2) had the medial to lateral direction but the other two (r1 and r2) had reversed propagating direction. One cycle, *S*, appeared to occur simultaneously on both detectors. Signals were filtered between 3–80 Hz.

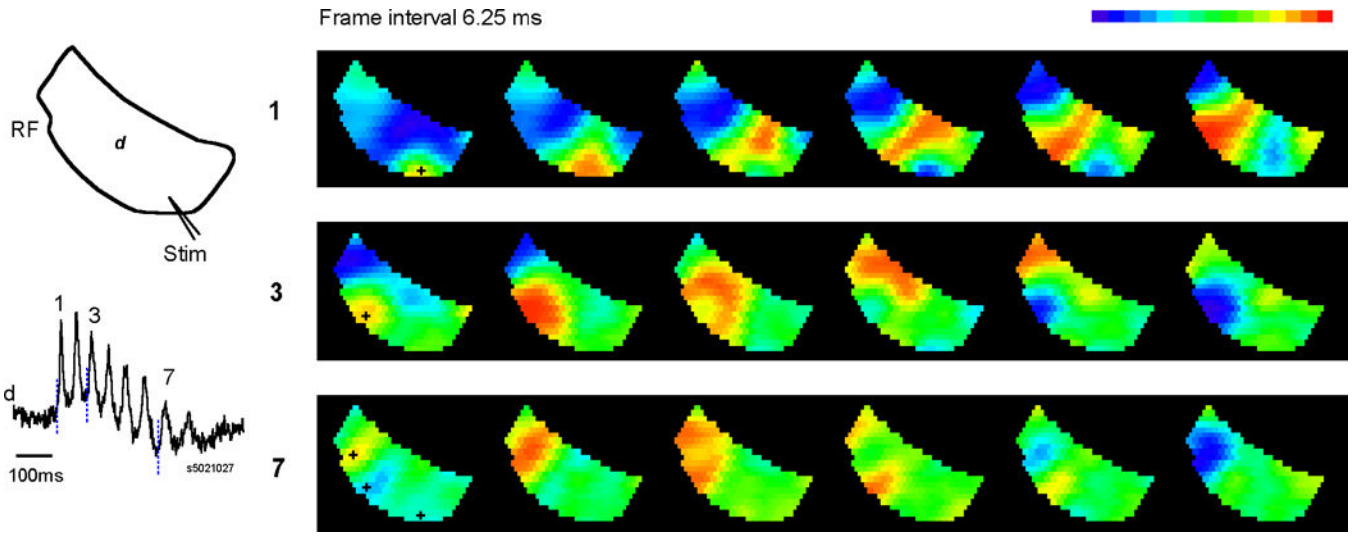

Figure 5.

Initiation foci of the waves. ***Left:*** The orientation of the slice and stimulation site is illustrated on the top. The signal from one optical detector, *d*, is shown on the bottom. The images of three oscillation cycles (1,3,7) are shown on the right panel. ***Right:*** Pseudo-color images generated from the signals of all optical detectors, with signal amplitude colored according to a linear pseudo-color scale (top right, peak to red and valley to blue). All images are snap shot of 0.625 ms and the interval between images are 6.25 ms. Each row of the images started at the time marked by a vertical broken line in the trace on the left panel. The initiation site was determined as the detector with earliest onset time and marked as black crosses in the first images of each row. The first spike (1) initiated at the location of stimulating electrode and propagated as a wave to the lateral (top row). Two of the following oscillation cycles (*3* and *7*) initiated from two different locations. All three initiation foci are marked at the first image of the bottom row for comparison. This optical recording trial contains 1100 images (~0. 7 sec) and only a few of them are shown for clarity. Movies with this type of images are included in the supplemental material.

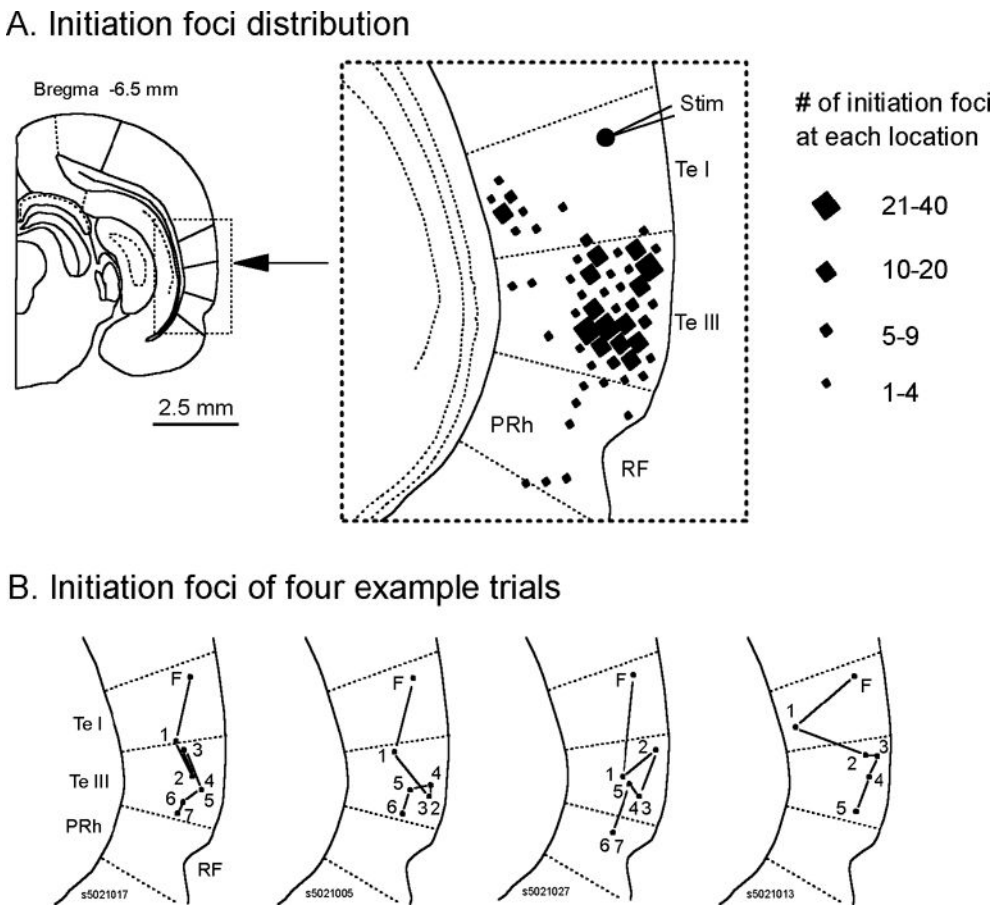

Figure 6.

Distribution of the initiation foci. ***A.*** Spatial distribution of the initiation foci of 352 oscillation cycles (first spike excluded) in one representative slice. The location of each focus is labeled by a diamond shaped mark. The size of the diamond mark represents the repeating occurrence at the each location (numbers at the right). The first spike always started at stimulation site (the round dot). All the subsequent oscillation cycles were not initiated near the stimulation site. The majority of the initiation foci are located in temporal cortex III area and a large portion of them was clustered at a few locations (larger diamonds). ***B.*** Initiation foci of four example trials from the slice shown in A. Numbers (1–7) indicate the sequence of the cycles following the first spike. While in all trials the first spike initiated at the same location (F, the stimulation site), the subsequent oscillation cycles were apparently initiated from randomly distributed locations.

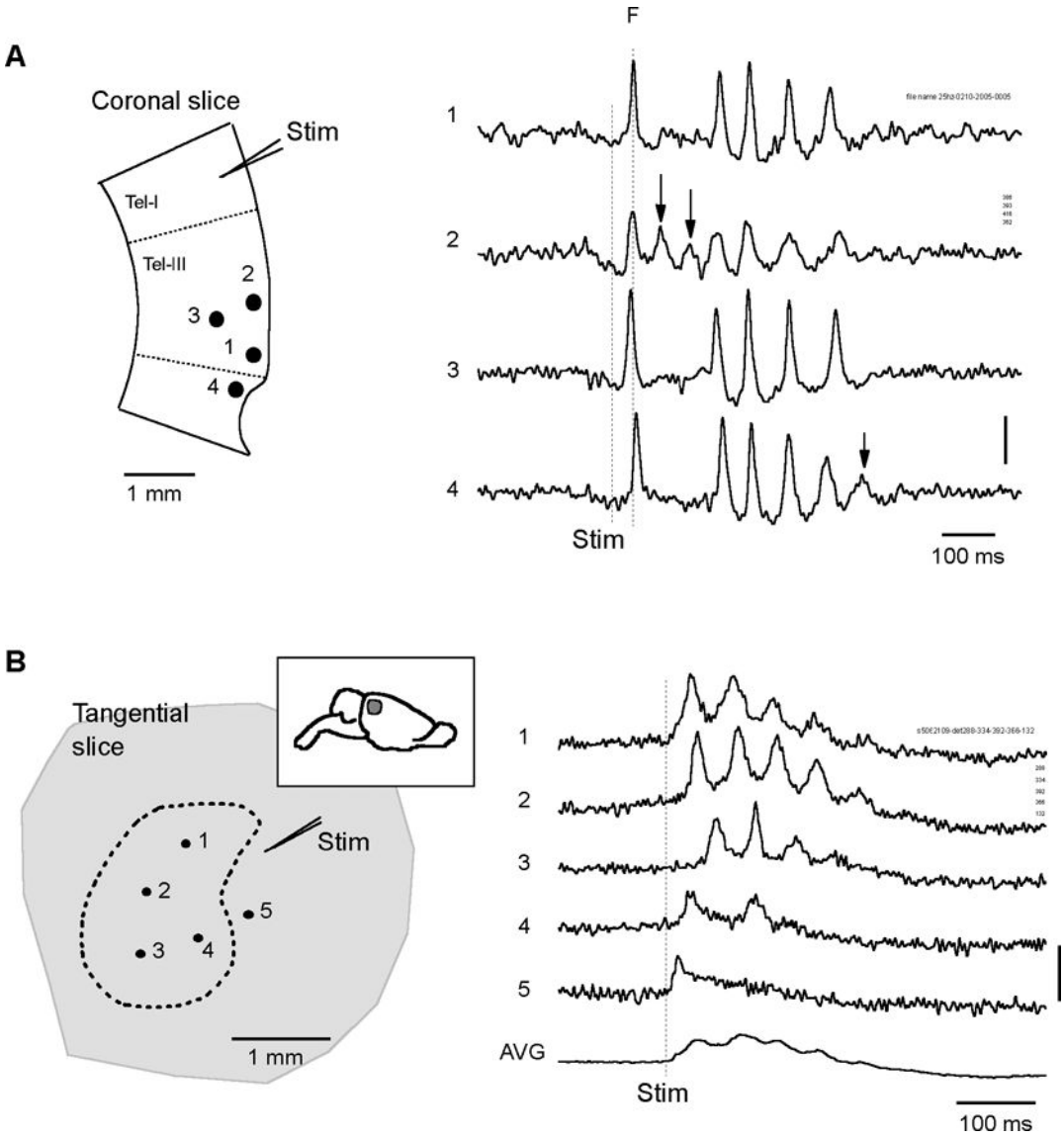

Figure 7.

Waveform variations over space. ***A.*** The voltage sensitive dye signals at four locations in a coronal slice (1–4, left) are shown (1–4, right). The first spike (broken line *F*) is seen at all locations. Extra oscillation cycles are seen at locations 2 and 4 (arrowheads). Signals are filtered between 3 – 200 Hz. Vertical scale: 2×10^{-4} of resting light intensity. ***B.*** An example of oscillations in tangential slices. ***Left***, The slice was sectioned parallel to the cortical surface, 500 μm thick including part of layer II–III and IV (location of the slice shown on the insert). Oscillations were seen in an area marked by the dashed line on about ~160 detectors. Traces from five detectors (1–5) are shown on the right. ***Right***, At different locations (1 – 4) there are different number of cycles. Outside the boundary of the dashed line there was only the first spike but no subsequent oscillation cycles (trace 5 on the right). Trace *AVG*, an average of all the ~160 detectors show largely reduced oscillation amplitude, suggesting the whole population was not synchronized. Vertical scale: 2×10^{-4} of resting light intensity. Signals are filtered between 1 – 200 Hz.

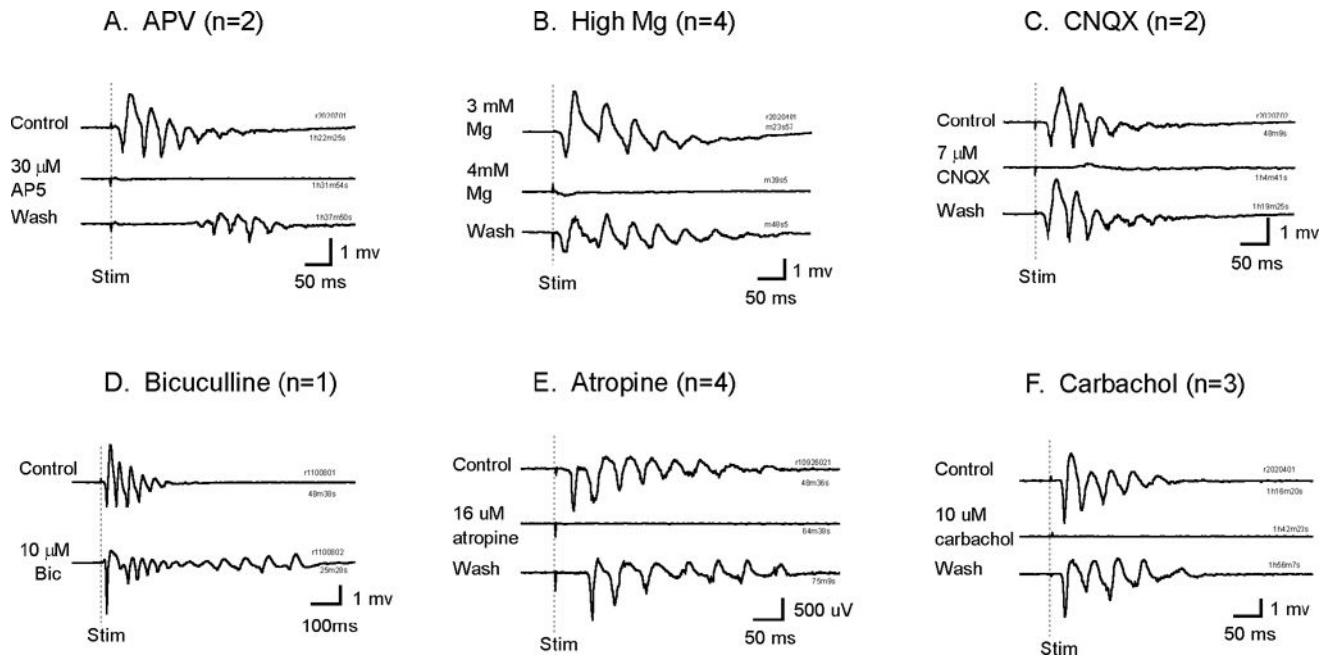

Figure 8.

Local field potential recordings of the oscillations under pharmacological manipulations. Blockade of NMDA receptors *(A, B)* and AMPA receptors *(C)* reversibly block the oscillations. Blocking $GABA_A$ receptors *(D)* did not abolish the oscillations. Manipulation of muscarinic/nicotinic receptors with atropine *(E)* or carbachol *(F)* reversibly block the oscillations. All drugs were added to the perfusing ACSF. The perfusion rate was ~ 20 ml/min (28°C). n is the number of animals, for each animal 2 to 3 slices were tested.

Table 1

Previous reported oscillations in brain slices

	Conditions	Frequency	Brain area	Duration
I	Zero or low Mg^{2+}	7–10 Hz	Hippocampus[1], cortex[2]	Long episodes
II	Carbachol/Kainate	~40 Hz	Hippocampus[3], cortex[4]	Continuous
III	Carbachol/bicuculline	4–15 Hz	Cortex[5]	Long episodes
IV	Evoked in normal ACSF	20–80 Hz	Cortex[6]	Short episodes
V	Spontaneous	6–10 Hz	Thalamus[7]	Short episodes
VI	Tonic stimulation	~40 Hz	Hippocampus[8]	Short episodes
VII	Transient K^+ elevation	50–80 Hz	Hippocampus[9]	Long episodes

Notes:

[1] Anderson et al., 1986;

[2] Silva et al., 1991, Flint et al., 1996;

[3] Fisahn et al., 1998, Dickinson et al., 2003;

[4] Buhl et al., 1998; Cunningham et al., 2003;

[5] Lukatch and MacIver, 1997;

[6] Luhmann and Prince, 1990; Metherate and Cruikshank, 1999;

[7] Kim et al., 1995;

[8] Whittington et al., 1995;

[9] Towers et al., 2002.